Journal of the Korean Physical Society, Vol. 50, No. 3, March 2007, pp. 622∼625

# Al-ZnO Thin Films as Transparent Conductive Oxides : Synthesis, Characterization, and Application Tests

Seong Hun JEONG,* Bit Na PARK, Dong-Geun YOO and Jin-Hyo BOO†
*Department of Chemistry and Institute of Basic Science, Sungkyunkwan University, Suwon 440-746*

Donggeun JUNG
*Department of Physics and Institute of Basic Science, Sungkyunkwan University, Suwon 440-746*

(Received 6 September 2006)

We have deposited an Al doped ZnO (AZO) film at room temperature by RF magnetron sputtering with homemade targets. We investigated the dependences of the optical and the electrical properties of the sputtered AZO films on the dopant contents in the targets. The AZO films should a preferred orientation in the [001] direction. As the amounts of the dopants were changed, the crystalline and the transmittance changed. The electrical resistivity also changed with changing aluminum doping amounts. The AZO films were used as anode electrodes for organic light-emitting-diode (OLED) devices.

PACS numbers: 81.15.Cd, 61.72.Vv, 85.30.-z, 85.60.Dw
Keywords: Transparent conductive oxide, Al-doped ZnO, OLED, Anode, RF magnetron sputtering

## I. INTRODUCTION

Zinc oxide is recognized as a semiconductors because it has a wide band gap of 3.37 eV at room temperature, a large free exciton binding energy (60 meV), and high mechanical and thermal stabilities. Generally, undoped ZnO thin films typically exhibit n-type conduction. It is caused by a deviation from stoichiometry due to native defects, such as oxygen vacancies or zinc interstitials [1]. Specially, an Al-doped ZnO (AZO) transparent conductive oxide (TCO) film has high transmittance in the visible region, and a low resistivity, and the optical bandgap can be controlled by the using Al doping amount [2,3]. ZnO TCO films are widely used in high, and low-tech applications, such as antistatic coatings, touch display panels, solar cells, flat panel displays, heaters, defrosters, and optical coatings. All these applications use the TCO as a simple passive electrical or optical coating [4]. Different methods are used to fabricated AZO thin films, the most common being: magnetron sputtering [5,6], pulsed laser deposition [7], chemical vapor deposition [8], and chemical spray [9], among others.

In this work, we investigate the effect of the aluminum concentration on the structural, the electrical, and the optical properties of AZO thin films deposited on glass substrates at different target-to-substrate distance (Dts) by RF magnetron sputtering. Moreover, the AZO films were used as an anode material for organic-light-emitting-diode (OLED) devices.

*Corresponding Author: niobium@skku.edu;
†Corresponding Author: jhboo@skku.edu;
Tel: +82-31-290-7072; Fax: +82-31-290-7075;
Department of Chemistry, Sungkyunkwan University, Suwon 440-746

## II. EXPERIMENT

### 1. ZnO Films Deposition and Characterization

Sintered oxide ceramic targets of ZnO (purity : 99.999 %, diameter : 2 inches) mixed with 2, 4, 6, 8, and 10 wt% $Al(OH)_3$ (purity 99.999 %) were fabricated. The AZO films were deposited on glass substrates at room temperature (RT) with an rf power of 200 W at different Dts and were used targets. Due to the practical applicability of AZO films, 150 $\sim$ 200 nm thick films were prepared on glass substrates. The general morphologies and cross sections of the AZO films were observed using field-emission scanning electron microscope (FESEM). Their crystallinity was investigated using X-ray diffraction (XRD). X-ray photoelectron spectroscopy (XPS) and energy dispersive X-ray spectroscopy (EDX) were also utilized to analyze the chemical ratios of AZO films. The optical transmittance measurements were performed with an UV/visible spectrophotometer. The sheet resistance ($R_s$) was determined by using four-point probe measurements. By assuming that the thickness of the films was uniform, we could calculate the film

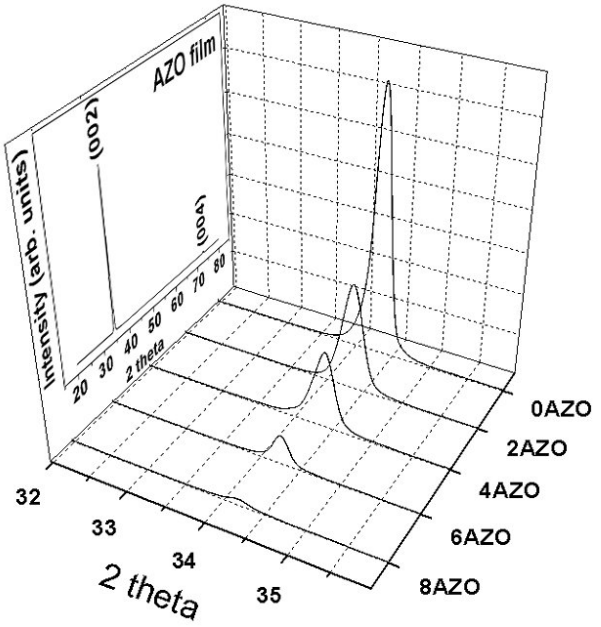


Fig. 1. XRD spectra measured for AZO films as a function of $Al(OH)_3$ content in the target. The insert of figure shows a typical XRD pattern of an AZO film.

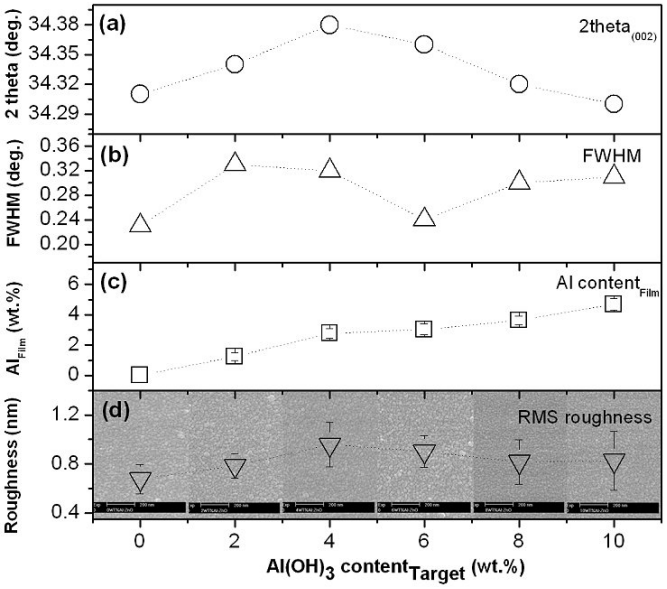


Fig. 2. AZO (a) (002) peak position, (b) FWHM, (c) Al concentration in the film, and (d) RMS roughness as functions of the $Al(OH)_3$ content in the target. The insets of (d) show the SEM morphologies of the AZO film as a function of the $Al(OH)_3$ content in the target.

resistivity($\rho$) by using the simple relation $\rho = Rs \cdot t$, where $t$ is the film thickness.

### 2. OLED Device Fabrication and Characterization

We used the AZO thin films as anodes for OLED devices. The device structure consisted of Al as the cathode, an ultra-thin $Al_2O_3$ layer, tris(8-hydroxyquinolinolato)aluminum(III) ($Alq_3$) as the luminous layer, and triphenyldiamine (TPD) as the hole transport layer. The current-voltage-brightness ($I$-$V$-$B$) data were taken using a current/voltage source and a brightness meter.

## III. RESULTS AND DISCUSSION

In previous research [10], we studied the influence of the Dts on various properties of the AZO films. The AZO films were deposited on glass at room temperature and an rf power of 150 W. The working environment consisted mainly of high-purity Ar (99.99 %) gas at 38 mTorr. In sum, the AZO films had low resistivity at a Dts of 45 mm owing to the non-stoichiometric films. Therefore, we studied the effect of the amount of aluminum quantity in the AZO films on the structural, the optical, the electrical, and the electronic properties of the TCO films.

### 1. Structural Characterization

Typical X-ray diffraction patterns of the AZO films, as shown in the inset of Fig. 1 with only the (002) peaks at $2\theta \approx 34°$, were observed for all samples. The measurements were taken at the central region of the samples. Fig. 1 illustrated that the (002) reflection was the prominent plane for AZO films prepared by sputtering targets of various ratios. This indicates an oriented film growth, with the crystallographic $c$-axes perpendicular to the substrate surface. Fig. 2 shows the $2theta_{(002)}$, the FWHM, the Al $content_{Film}$, the RMS roughness, and the surface morphology as functions of the Al concentration. The films deposited at room temperature exhibit only (002) peak in the displayed 2 theta region, no metallic Zn or Al characteristic peaks were observed. This may be due to aluminum replacing zinc substitutionally in the hexagonal lattice ($Al_{Zn}$) or aluminum segregating to the non-crystalline region in the grain boundary ($Al_{Boundary}$). The location of the diffraction pattern peaks shifted slightly to high diffraction angle with increasing Al quantity (until 4 wt.%), and the intensity of these peaks became weaker (until 8 wt.%) and broader (until 6 wt.%). The lowest FWHM value (see Fig. 2(b)) was 0.24° for the ZnO film deposited using a 6 wt.% AZO target. The broadened peak means the defect site is in the lattice, which means an oxygen vacancy or an interstitial zinc. The thin films deposited using 4 wt.% AZO target had the highest (002) peak shift; more Al was incorporated into the lattice. However, the highest Al quantity was 4.71 wt.% in the film

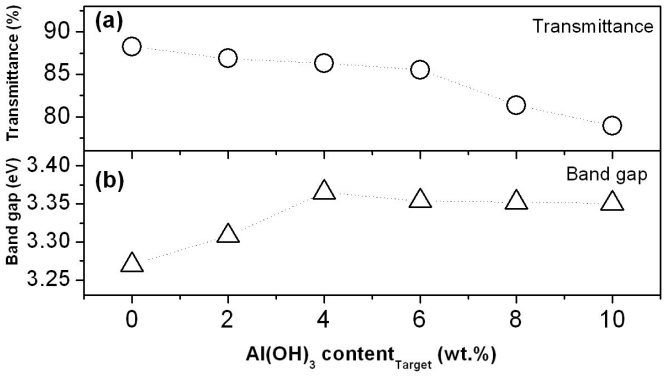


Fig. 3. Wavelength-dependent optical transmittance and optical band gap of AZO films as functions of the $Al(OH)_3$ content in the target.

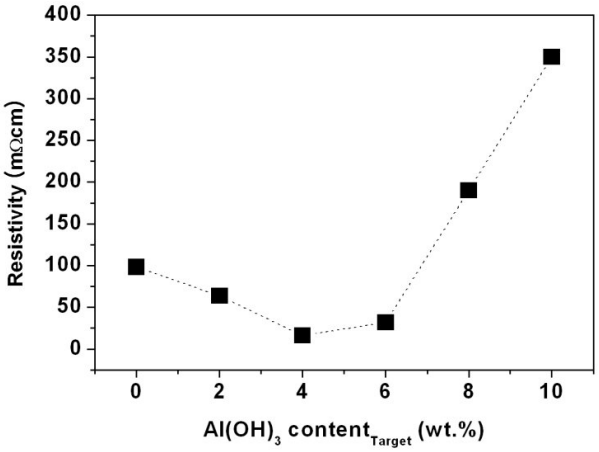


Fig. 4. Resistivity of AZO films as a function of the $Al(OH)_3$ content in the target.

using 10 wt.% AZO target (see Fig. 2(c)). Much Al was located in the grain boundary, but this aluminum did not influence the resistivity of thin film. Fig. 2(d) shows SEM morphologies of the AZO films prepared by using preparatory targets at room temperature. As the Al concentration increased, the grain size decreased, and the surface roughness increased slightly (until 4 wt.% AZO). This result, in agreement with the XRD result, indicates that aluminum substituted at the zinc site. The surface roughness decreased with increasing Al concentration (until 10 wt.% AZO) because Al segregated to the non-crystalline region in the boundary.

### 2. Optical Properties

The average transmittance values as function of wavelength in the range of $400 - 800$ nm for the samples are shown in Fig. 3(a). As the Al concentration increased, the average transmittance decreased. Song *et al.* [3] reported that the transmittance might be attributed to an increase in the free-carrier concentration. Therefore, a lower resistivity and a higher transmission in the visible range are not entirely compatible. However, aluminum divided into two classes in the thin films ($Al_{Zn}$ and $Al_{Boundary}$). Perhaps, among others, $Al_{Zn}$ in the doping aluminum might be attributed to the effect of the free-carrier concentration in the thin film. The optical band gap (Eg) of the thin films could be obtained by plotting $\alpha^2$ vs. $h\nu$, ($\alpha$ is the absorption coefficient and h$\nu$ is the photon energy) and extrapolating the straight line portion of this plot to the energy axis. From Fig. 3(b), Eg for pure ZnO film is 3.27, and $3.31 - 3.35$ eV was obtained for AZO films prepared with preparatory targets, which is larger than that of pure ZnO due to the Burstein shift. The broadening of band gap with increasing Al concentration might be due to an increased carrier density.

### 3. Electrical Properties

Fig. 4 gives the aluminum concentration dependence of the resistivities for the AZO thin films on glass substrates. These films were deposited at room temperature with the Dts = 45 mm by using various prepared AZO targets. As the Al concentration in the target increased, the electrical resistivity decreased and reached a minimum value of 16 m$\Omega$cm for a 4 wt.% $Al(OH)_3$-doped zinc oxide target. In comparison with previous structural and optical characteristic, Al substituted at zinc sites in the hexagonal lattice or aluminum segregated to the non-crystalline region in the grain boundary. $Al_{Zn}$ in the doping aluminum might be attributed to the effect of the free-carrier concentration in the thin film. Therefore, $Al_{Zn}$ has an influence on the electrical resistivity, but $Al_{Boundary}$ does not.

### 4. OLED Device Performance

The AZO films prepared using 4 and 6 wt.% Al-doped ZnO targets were employed as anode contacts in OLEDs. Both OLEDs had active emitting areas of 2 mm $\times$ 2 mm on glass. Figs. 5(a)-(d) show the current density, luminance, quantum efficiency, and luminance efficiency of the OLEDs as functions of the operating voltage, *i.e.*, J-V, L-V, QE-V, and LE-V plots. The curves with triangles and inverted triangles plotted in Fig. 5 correspond to the device characteristics obtained from OLEDs made with AZO anodes prepared using 4 and 6 wt.% AZO targets, respectively. We obtained the lowest turn-on voltages at a value of 5.5 V and a good luminance (10500 cd/m$^2$) of the light emitted form the OLEDs using 4AZO anodes. However, the OLED device prepared using the 4AZO target had electrical leakage because of a structural defect in the range of operating voltage from $0 - 7$ V, but the current density for the AZO-anode diodes was

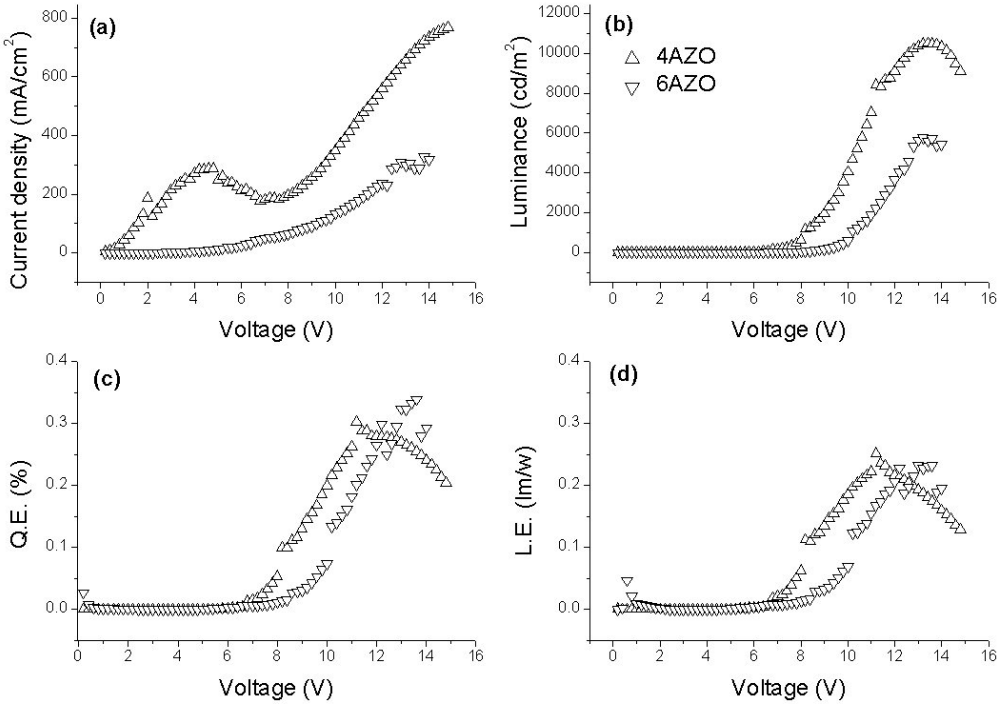


Fig. 5. (a) Current density, (b) luminance, (c) quantum efficiency, and (d) luminance efficiency for AZO-based OLEDs.

much lower that that for the ITO-anode devices. This resulted from work function and the carrier concentration of the used AZO films being lower than those of the used ITO films [11].

## IV. CONCLUTIONS

Transparent conducting AZO thin films were deposited on glass substrates by rf magnetron sputtering using various prepared AZO targets at room temperature. Highly-oriented ZnO thin films in the [001] direction were grown. AZO films with the transmittances of over 85 % in the visible region and an electrical resistivity of 16 mΩcm were obtained at Dts of 45 mm by using a 4 wt.% AZO target. The AZO films (4AZO, 6AZO) were used as anode contacts to fabricate OLEDs devices. The lowest turn-on voltage at 10500 cd/m$^2$ was 5.5 V for the devices with the 4AZO anode, and the quantum efficiency was 0.3 %. This work demonstrates that an AZO film deposited at a low processing temperature may serve as an alternative TCO material to ITO for OLED devices.

## ACKNOWLEDGMENTS

Support for this research by the BK 21 project of the Ministry of Education, Korea, is gratefully acknowledged and by the Korea Research Foundation Grant funded by the Korean Government (MOEHRD, KRF-2005-005-J11902). This work was supported by the Faculty Research Fund, Sungkyunkwan University, 2005, and by the SAIT/SAINT joint project.

## REFERENCES

[1] S. Major and K. L. Chopra, Sol. Energy Mater. **17**, 319 (1998).
[2] K. C. Park, D. Y. Ma and K. H. Kim, Thin Solid Films **305**, 201 (1997).
[3] J.-Y. Hwang, C.-R. Cho, S.-A. Lee and S.-Y. Jeong, J. Korean Phys. Soc. **47**, S288 (2005).
[4] J. F. Wager, Science **300**, 1245 (2003).
[5] Z. Le and W.Gao, Materals Letters **58**, 1363 (2004).
[6] X.-T. Hao, L.-W. Tan, K.-S. Ong and F. Zhu, J. Cryst. Growth **287**, 44 (2006).
[7] J. H. Jo, T.-B. Hur, J. S. Kwak, D. Y. Kwon, Y.-H. Hwang and H. K. Kim, J. Korean Phys. Soc. **47**, S300 (2005).
[8] Y. Natsume, H. Sakata, T. Hirayama and H. Yanagada, J. Appl. Phys. **72**, 4203 (1992).
[9] H. Mondragon-Suarez, A. Maldonaldo, M. de la L. Olvera, A. Reyes, R. Castanedo-Perez, G. Torres-Delgado and R. Asomoza, Appl. Surf. Sci. **193**, 52 (2002).
[10] S.H. Jeong, J.-H. Boo, Thin Solid Films **447-448**, 105 (2004).
[11] D. Xu, Z. Deng, Y. Xu, J. Xiao, C. Liang, Z. Pei and C. Sun, Phys. Lett. A **346**, 148 (2005).